AGU PUBLICATIONS

Earth's Future

RESEARCH ARTICLE
10.1002/2017EF000607

Special Section:
Avoiding Disasters: Strengthening Societal Resilience to Natural Hazards

Deep Uncertainty Surrounding Coastal Flood Risk Projections: A Case Study for New Orleans

Tony E. Wong[1] **and Klaus Keller**[1,2,3]

[1]Earth and Environmental Systems Institute, Pennsylvania State University, University Park, Pennsylvania, USA, [2]Department of Geosciences, Pennsylvania State University, University Park, Pennsylvania, USA, [3]Department of Engineering and Public Policy, Carnegie Mellon University, Pittsburgh, Pennsylvania, USA

Abstract Future sea-level rise drives severe risks for many coastal communities. Strategies to manage these risks hinge on a sound characterization of the uncertainties. For example, recent studies suggest that large fractions of the Antarctic ice sheet (AIS) may rapidly disintegrate in response to rising global temperatures, leading to potentially several meters of sea-level rise during the next few centuries. It is deeply uncertain, for example, whether such an AIS disintegration will be triggered, how much this would increase sea-level rise, whether extreme storm surges intensify in a warming climate, or which emissions pathway future societies will choose. Here, we assess the impacts of these deep uncertainties on projected flooding probabilities for a levee ring in New Orleans, LA. We use 18 scenarios, presenting probabilistic projections within each one, to sample key deeply uncertain future projections of sea-level rise, radiative forcing pathways, storm surge characterization, and contributions from rapid AIS mass loss. The implications of these deep uncertainties for projected flood risk are thus characterized by a set of 18 probability distribution functions. We use a global sensitivity analysis to assess which mechanisms contribute to uncertainty in projected flood risk over the course of a 50-year design life. In line with previous work, we find that the uncertain storm surge drives the most substantial risk, followed by general AIS dynamics, in our simple model for future flood risk for New Orleans.

Key Points:
- We characterize key deep uncertainties surrounding flood risk projections for a levee ring in New Orleans using 18 probabilistic scenarios
- The levee system alone may provide flood protection between the 100- and 500-year return period
- Uncertainty in the storm surge distribution shape parameter is the primary driver of flood risk variability

Supporting Information:
- Supporting Information S1

Corresponding author:
T. E. Wong, anthony.e.wong@colorado.edu

Citation:
Wong, T. E., & Keller, K. (2017). Deep uncertainty surrounding coastal flood risk projections: a case study for new orleans, *Earth's Future*, *5*, 1015–1026, https://doi.org/10.1002/2017EF000607

Received 2 MAY 2017
Accepted 12 SEP 2017
Accepted article online 20 SEP 2017
Published online 10 OCT 2017

1. Introduction

Sea-level rise poses nontrivial risks to coastal communities (Nicholls & Cazenave, 2010; Hallegatte et al., 2013; Hinkel et al., 2014; Hinkel et al., 2015). The performance of strategies to manage these risks relies on sound projections of future sea levels and storm surges, including the inherent uncertainties (cf. Hinkel et al., 2015).

In a comparison of projected future flood losses in 136 coastal cities across the world, recent work has found that New Orleans, LA, ranks second in average annual loss (as percentage of the city's gross domestic product), even with adaptation to maintain present flood risk (Hallegatte et al., 2013). Another recent study found substantially higher estimates for the average annual losses faced by New Orleans (Abadie et al., 2017), where the discrepancy between the two studies is driven by the higher projected sea-level rise used in the latter study (Kopp et al., 2014). The United States Army Corps of Engineers (USACE) has stated its objective to develop coastal defense strategies (including for New Orleans) that perform well across a range of plausible climate change scenarios (Moritz et al., 2015). However, recent scientific findings suggest that future flood risks may be higher and more uncertain than previously estimated (e.g., Grinsted et al., 2013; DeConto & Pollard, 2016; Abadie et al., 2017; Bakker et al., 2017; Wong et al., 2017a). Here, we assess the expected performance of the flood protection system in New Orleans under a set of plausible future climate scenarios that account for key new scientific findings and sample key deep uncertainties. We caution that our intent is to attribute and characterize the impacts of these deep uncertainties, which are not meant to directly inform on-the-ground decisions.

Deep uncertainty refers to the situation in which experts cannot agree on the set of possible outcomes, the consequences of those outcomes, and/or the associated probabilities (e.g., Langlois & Cosgel, 1993; Walker et al., 2013). In these cases, the use of a range of plausible future scenarios or multiple probability density functions (PDFs) can provide useful inputs for the design of risk management strategies (e.g., Schoemaker, 1993; Bryant & Lempert, 2010; Lempert et al., 2012). Such a representation of uncertainties can be critical to

inform decision making, for example, in the context of coastal risk management (De Winter et al., 2017). The presentation of multiple scenario PDFs enables the identification of scenarios to which particular strategies may be vulnerable and enables decision makers to determine the appropriate protective action in the face of these vulnerabilities (e.g., Lempert et al., 2012). Furthermore, using multiple PDFs can provide a traceable combination of information from diverse sources containing differing levels of uncertainty (Lempert et al., 2012) and characterizes the impacts of deep uncertainty on possible future outcomes (Oppenheimer & Alley, 2016).

The deeply uncertain future radiative forcing is often represented in the form of Representative Concentration Pathways (RCP) scenarios (Meinshausen et al., 2011). These scenarios may be used to link radiative forcing to the consequent changes in local sea levels and, finally, to their implications for coastal defense strategies (Jackson & Jevrejeva, 2016; Wong et al., 2017a). Uncertainty in future storm surge severity also drives substantial risks to coastal communities (Resio et al., 2013). Previous approaches to project future storm surges have included physical modeling (e.g., Orton et al., 2016), statistical modeling (e.g., Grinsted et al., 2013), and scenarios (e.g., Lempert et al., 2012; Johnson et al., 2013). Here, we expand upon and combine these approaches by providing probabilistic scenarios of future storm surge level. Potential fast Antarctic ice sheet (AIS) disintegration via cliff instability and hydrofracturing in response to rising global temperatures is a critical deep uncertainty, driving potentially large changes in sea-level rise this century (DeConto & Pollard, 2016; Oppenheimer & Alley, 2016; Bakker et al., 2017; Ruckert et al., 2017; Wong et al., 2017a). Recent work projecting this fast dynamical Antarctic contribution to sea level used radiative forcing scenarios (Meinshausen et al., 2011) as well as multiple prior distributions on key model parameters to provide probabilistic ranges within each scenario (Wong et al., 2017a). Other recent studies employed statistical approaches based on the projections of DeConto and Pollard (2016) to construct probabilistic projections of the rapid Antarctic mass loss (Kopp et al., 2017; Le Bars et al., 2017). Here, we employ the mechanistically motivated emulator of Wong et al. (2017a) to construct our projections of future Antarctic contributions to sea level. This model choice is motivated by (1) our intention to explicitly represent deeply uncertain geophysical mechanisms (e.g., the triggering of Antarctic fast ice loss) and connect these to local flood risk and (2) a successful hindcast test (Wong et al., 2017a). We caution, however, that passing a hindcast test (e.g., DeConto & Pollard, 2016; Wong et al., 2017a) is, of course, no guarantee that a model will capture future dynamics, especially when the physical system in question is as deeply uncertain and nonlinear as the AIS.

There are, of course, other deep uncertainties affecting flood risk that could be taken into account in future work. These include potential rapid ice melt/disintegration from the Greenland ice sheet and more complex basin-scale Antarctic dynamics (Ritz et al., 2015), as well as potential feedbacks and correlations among the deeply uncertain factors considered here (e.g., between RCP scenario and storm surge nonstationarity). The fragility of the flood protection system may also be considered a deeply uncertain factor, for example, to bound the probability of failure (Johnson et al., 2013). In this study, we consider only the overtopping levee failure mechanism. This provides a reasonable estimate of a lower bound on the failure probability. This serves to simplify the analysis and leaves the treatment of levee reach-scale failure properties to more detailed analyses (e.g., Fischbach et al., 2012).

Here, we provide probabilistic projections of flood risk for the city of New Orleans, conditioned on the deeply uncertain scenarios detailed above. Specifically, we consider multiple future scenarios spanning radiative forcing, fast AIS disintegration, and characterization of future storm surges. We expand upon previous work by providing a probabilistic accounting of both stationary and nonstationary storm surge characteristics, as well as putting recent scientific findings—the potential fast AIS dynamic mass loss contributions to sea-level rise—into a local coastal protection context. We use global sensitivity analysis (Sobol', 2001) to identify the key modeling uncertainties that drive uncertainty in future flood risk. The scope of this work is limited to the characterization and attribution of the impacts of deeply uncertain geophysical drivers on uncertainty in projected flood risk. The purpose of this work is (1) to provide a menu of plausible probabilistic scenarios of future flood risk for New Orleans, (2) highlight primary drivers of flood risk, and (3) to incorporate the newly available probabilistic projections of the fast AIS contribution to sea levels into the flood risk assessment.

2. Methods

2.1. Sea-Level Rise

We simulate global mean surface temperature, ocean heat uptake, and global mean sea level and its contributions from the AIS, Greenland ice sheet, thermal expansion, glaciers and ice caps, and land water storage using the Building Blocks for Relevant Ice and Climate Knowledge (BRICK) model v0.2 (Wong et al., 2017b) with a modified AIS fast dynamics emulator (Wong et al., 2017a). BRICK is an open-source platform of semiempirical models for the major contributions to global mean sea level. We calibrate the model preferentially to observational records as opposed to simulation output from more complex models. The model set-up, calibration to paleoclimate and instrumental data, and simulations proceed as described in Wong et al. (2017a). We run the model from 1850 to 2065. We use 2065 as the time horizon for analysis in light of the 50-year planning horizon implemented in the Louisiana Coastal Protection Master Plan (p. 48, Coastal Protection and Restoration Authority (CPRA), 2017). Sea-level rise is presented relative to sea level in 2015. We use historical radiative forcing (described by Urban & Keller, 2010) and observational data between 1850 and 2009 to calibrate the model (Wong et al., 2017b). The model is then run from 1850 to 2065 under the RCP2.6, 4.5, and 8.5 radiative forcing scenarios (Meinshausen et al., 2011). Thus, there are three scenario cases for radiative forcing. Local scaling factors are used to estimate the local mean sea-level rise in New Orleans from the simulated contributions to global sea level from glaciers and ice caps, the Greenland ice sheet, the AIS, thermal expansion, and land water storage (Slangen et al., 2014; Wong et al., 2017b). We sample the effects of land subsidence on local sea level around a recent estimate (Dixon et al., 2006) (see Section 2.3). All sea levels presented are New Orleans local sea level.

Recent work has shown that ice cliff instability and hydrofracturing may lead to substantial and rapid contributions from the AIS to sea-level rise (DeConto & Pollard, 2016). We employ the following emulator for the contribution of these fast AIS dynamics to global mean sea level:

$$\frac{dV}{dt} = \begin{cases} -\lambda, & T > T_{crit} \\ 0, & T \leq T_{crit} \end{cases}, \qquad (1)$$

where λ is an uncertain rate of disintegration (mm year^{-1}), T_{crit} is the threshold temperature at which fast dynamical disintegration is triggered (°C), and T is the mean Antarctic surface temperature reduced to sea level (Diaz & Keller, 2016; Wong et al., 2017a).

The parameters λ and T_{crit}, along with 39 other BRICK model parameters, are jointly estimated within a Bayesian calibration framework (Wong et al., 2017b). We include three scenarios for the potential AIS fast dynamics: "*gamma*", "*uniform*", and "*none*". In the "*gamma*" and "*uniform*" scenarios, the prior distributions assumed for the fast dynamics parameters λ and T_{crit} are assumed to be gamma or uniform distributions, respectively (Wong et al., 2017a). The effect of the gamma prior distribution is to put more weight on central values of these parameters, with ranges informed by the literature (DeConto & Pollard, 2016). Each of these two sets of prior distributions yields an ensemble of calibrated projections of future sea level, including the additional sea-level contributions from the AIS fast dynamics. These ensembles each contain 12,586 states of the world (SOW) and are simulated under each of the three radiative forcing scenarios.

The ensemble of simulations for the third AIS fast dynamics scenario, "*none*", is drawn from the *gamma* and *uniform* ensembles (6293 simulations each), neglecting the contributions of the AIS fast dynamics to sea level. The three AIS fast dynamics scenarios span a range of possible outcomes for the fast dynamical AIS contributions to sea level in this century—*none*, AIS disintegration does not occur; *uniform*—we possess enough information to bound the values of the parameters driving disintegration; and *gamma*—we possess a high degree of confidence in our prior beliefs regarding the disintegration parameterization. We run each of these three AIS fast dynamics scenarios under each of the three radiative forcing scenarios. This yields a total of nine sea-level rise scenarios.

2.2. Storm Surge

We use tide gauge data from Grand Isle, Louisiana, and a Bayesian calibration approach to fit an ensemble of stationary generalized extreme value (GEV) distributions for the storm surge level (NOAA, 2017). The hourly tide gauge data span the period from November 1980 to December 2016. First, we subtract annual

means from the tide gauge record. Second, we calculate annual block maxima from the detrended record. Third, we calculate a maximum likelihood estimate for the GEV distribution parameters, fit to the tide gauge data (see Text S1, Supporting Information). Fourth, we use the resulting estimate as the starting point for two 500,000-iteration Markov chain Monte Carlo simulations of the GEV parameters (see Text S1). Finally, we discard the first 100,000 iterations of each chain for "burn-in" (see Supporting Information) and draw an ensemble of 12,586 samples from the combined sample of 800,000 remaining chain members. The ensemble size is dictated by the size of the BRICK sea-level rise ensemble of simulations. The extreme value analysis described here is performed using the *extRemes* package in the R Programming Language (Gilleland et al., 2013; R Core Team, 2016). These 12,586 sets of GEV parameters are used to characterize the stationary (i.e., not time-varying) distribution of storm surge level in New Orleans for each of the radiative forcing/AIS fast dynamics scenario combinations. Thus, there are nine scenarios where the distribution of storm surge levels is assumed to remain stationary, characterized by their present values but accounting for uncertainty through the Markov chain Monte Carlo sampling.

We follow an approach outlined by the United States Army Corps of Engineers (USACE, 2012) to extrapolate the potential for nonstationary storm surge behavior from the stationary storm surge characterization and changes in future sea levels. Specifically, we project the increase in surge level as the product of the increase in sea level and an uncertain "surge factor", C_{surge}, which we sample uniformly between 1.5 and 2 (Table 1.2, USACE, 2012). The range of values for C_{surge} is based on a set of Advanced Circulation Model simulations, which were conducted to assess the effects of the increasing sea levels on surge heights (USACE, 2012). We calculate the nonstationary storm surge level as the sum of the storm surge level from the stationary GEV distribution and the increase in surge levels. Thus, a distribution for the increase in storm surge level provides a nonstationary storm surge characterization. This gives rise to nine scenarios (each of the radiative forcing and AIS fast dynamics combinations) with nonstationary storm surge, and a total of 18 scenarios.

Previous work has projected changes in future storm surge levels by fitting a nonstationary GEV distribution to a sizeable tide gauge record (Grinsted et al., 2013). Alas, the Grand Isle data set contains only 36 full years of data. The discussion in Grinsted et al. (2013) and preliminary experiments conducted here suggest that such a short record is not sufficient to constrain a fully nonstationary GEV model with high precision. Indeed, the nonstationary storm surge is comprised of two components, one driven by natural variability and the other driven by long-term climate changes. The former is likely poorly sampled in such a short tide gauge record. Thus, we follow the alternative approach described above (USACE, 2012). This approach misses potentially important processes, such as the reported influence of elevated temperatures on storm surge intensity (e.g., Grinsted et al., 2013) or changes in the Atlantic Meridional Overturning Circulation and upper ocean heat uptake (e.g., Little et al., 2015). Our simple approach does link sea-level changes (driven by changing global temperatures) to the simulated storm surge. In this approach, sea level can be viewed as a proxy for temperature in driving increased storm surge intensity (although increased temperature does not necessarily always lead to increased surge intensity); however, this approach still misses the potential changes in storm surge driven by mechanisms other than temperature.

2.3. Coastal Flood Risk

We focus on the north-central Metropolitan New Orleans levee ring. This levee system contains the East Jefferson and Orleans Metropolitan areas and has been the subject of previous studies (e.g., Jonkman et al., 2009; Wong et al., 2017a). We assume a levee ring average height of 4.88 m (16 ft) and an initial levee structure base elevation relative to local sea level of −1.22 m (−4 ft) (United States Army Corps of Engineers (USACE), 2014). That the base of the flood protection structure is negative indicates the effects of land subsidence. We sample uncertainty in future land subsidence by drawing 12,586 samples from a log-normal distribution with a mean of 5.6 mm year^{-1} and a standard deviation of 2.5 mm year^{-1} (Dixon et al., 2006), where the size of the ensemble is determined by the size of the BRICK sea-level rise ensemble of simulations.

Our method produces 18 probabilistic scenarios that include distributions of (1) sea-level rise, (2) land subsidence, (3) stationary storm surge, and (4) increase in surge level (for the non-stationary scenarios only). These scenarios are summarized in Table 1. We note that these scenarios do not cover the set of all possible futures and that the probabilistic projections within each scenario are conditionally dependent on the deeply uncertain storm surge, AIS fast dynamics, and RCP forcing, which do not have probability distributions assigned to them. Thus, these 18 scenarios serve to *characterize* key aspects of these deep

Table 1.
Deeply Uncertain Factors Sampled to Construct Scenarios

Radiative forcing	Antarctic fast dynamics	Storm surge
RCP2.6	None	Stationary
RCP4.5	Uniform prior PDF	Nonstationary
RCP8.5	Gamma prior PDF	

uncertainties as opposed to *quantifying* them. The total sea plus storm surge level that is incident on the flood protection system is the sum of these individual components. We focus our attention on these distributions of flood risk in the year 2065.

We calculate flood probabilities for each year as the tail area of the local mean sea plus storm surge level distribution above the levee height (reduced for the initial subsidence) to yield the annual exceedance probability. We estimate the return period as the inverse of the average annual exceedance probability. For example, the Coastal Protection and Restoration Authority of Louisiana has target protection levels of 1/100 annual exceedance probability (100-year return period) for general projects and 1/500 annual exceedance probability (500-year return period) suggested for critical infrastructure, such as hospitals and emergency response stations (p. 143, CPRA, 2017). Note that the flood probability in 2065 is almost certainly larger than the average annual exceedance probability due to temperature-driven increases in sea level and storm surge intensities (Grinsted et al., 2013; Kopp et al., 2016). Note further that the failure probabilities calculated here consider only the protection offered by the levee system; other adaptive and protective measures may increase the effective return period. Additionally, we only consider the overtopping failure mode at present. Levee failure modes such as piping and slope instability lead to an actual failure probability that is likely larger than the estimates presented here (see Section 4). Our analysis also does not account for the potentially sizable cumulative hazard arising from frequent minor flooding, or nuisance flooding (Moftakhari et al., 2017). As sea-level rise reduces the buffer between sea level and the flood stage, nuisance flooding is expected to become more frequent and more severe over the next few decades (Ray & Foster, 2016; Vandenberg-Rodes et al., 2016), and will likely surpass the 30 days year^{-1} tipping point by mid-century (Sweet & Park, 2014). This is, of course, an important avenue for continued study.

2.4. Sobol' Sensitivity Analysis

We employ an approach for global sensitivity analysis based on the method originally described by Sobol' (2001) and expanded by Saltelli (2002) and Janon et al. (2014). These works describe the Sobol' sensitivity analysis method in detail; we thus provide only a brief overview here. The approach decomposes the variance in a model response into components attributable to individual uncertain model parameters or forcings. We decompose the variance in the modeled mean annual exceedance probability (i.e., the flood risk) over the 2015–2065 period. We attribute the variance to uncertain endogenous model parameters (pertaining to land subsidence, storm surges, and changes in global temperature and the associated glacier, ice sheet, and ocean thermal responses), as well as to exogenous model forcings, including heightening of the levee system (by construction) and radiative forcing pathway (i.e., RCP scenario). We sample the RCP scenario uniformly from (0, 1), where each of four intervals of width 0.25 correspond to the scenarios RCP2.6, 4.5, 6.0, and 8.5. Levee heightening is sampled uniformly from −0.91 m to 0.91 m. This range is chosen to reflect current plans to heighten much of this levee system and the fact that the levee height is not uniform around the levee ring (e.g., Tables 3–8, USACE, 2014).

We calculate first-order Sobol' sensitivity indices (direct parameter/forcing influences on projected flood risk variance) and total sensitivity indices (the sum of the first- and all higher-order interaction indices for a particular term) for each parameter/forcing term and the second-order sensitivity indices (the impacts on flood risk of interactions between two parameters/forcings) for each parameter/forcing pair. We display the results for these sensitivity indices in a radial convergence diagram (Lima, 2011). In the radial convergence diagram, each parameter/forcing term is represented by a node around the perimeter of a circle, grouped by submodel components. The color of the node indicates a first-order (direct) influence on flood risk or total sensitivity (direct plus all indirect influences via parameter/forcing interactions). The size of each term's

node corresponds to the magnitude of the flood risk sensitivity to that term; larger nodes indicate greater sensitivity. Bars connecting nodes indicate that interactions between two terms are connected to flood risk variability; thicker bars indicate greater second-order sensitivity of flood risk to interactions between that parameter/forcing pair. Note that the sum of all of the first-, second-, third- (and so on) indices necessarily equals 100%. The sum of the total sensitivity indices, however, exceeds 100% due to multiple counting of the higher-order interactions among the parameters and forcings. The Supporting Information section provides a table containing the parameter and forcing term symbols and descriptions.

We construct an ensemble of 10,248,000 model realizations using model parameters drawn from the distributions resulting from the calibration to paleoclimate and instrumental data (as described in Wong et al., 2017a). We use bootstrap resampling to estimate confidence intervals for each sensitivity index. We select sample sizes to yield confidence intervals that are all <10% of the total sensitivity index for the leading index (Butler et al., 2014), using 50,000 bootstrap replicates. We only report sensitivity indices above a threshold of 1% of the total variance.

3. Results

3.1. Probabilistic Projections of Future Sea Level and Storm Surge

We characterize the deeply uncertain future sea and storm surge levels using probabilistic projections within each of the 18 scenarios (Figure 1). The impacts of the AIS fast dynamics on future sea level are noticeable in RCP4.5 and 8.5 at the 1/500 level (Figure 1c). At the 1/100 level, the AIS fast dynamics drive substantial sea-level changes by 2065 under RCP8.5 (Figure 1a and 1c). This conclusion is in line with the results of Wong et al. (2017a), who find a time horizon of 2060 (ensemble median) for the onset of fast dynamical AIS disintegration under RCP8.5. However, these effects are dwarfed by the projected increases in storm surge levels (Figure 1b and 1d).

The tail events in nonstationary storm surge threat are much larger than those from sea-level rise alone (i.e., low-probability but high-impact events such as fast AIS disintegration). At the 1/100 level, the AIS fast dynamics drive considerable increases in sea level in RCP8.5 (Figure 1c), but the risks posed by nonstationary storm surge at the 1/100 level are much higher (Figure 1d). This gives rise to the structure of Figure 2: fast AIS disintegration occurs in the most severe SOW, but the driving force behind high flood risk is the storm surge severity. In particular, the nonstationary storm surge scenarios lead to the highest flood risks (Figure 2b).

3.2. Potential Failure to Meet Flood Protection Standards

The 100-year flood protection standard (1/100 mean annual exceedance probability) (p. 143, CPRA, 2017) is achieved by the levee system alone in the ensemble median in all considered scenarios (Figure 3, solid red vertical line). However, a sizeable number of SOW in each scenario extend below the 100-year protection standard. The left-most extent of each scenario box in Figure 3 is the 25% quantile for that scenario's SOW. This implies that across all scenarios, the levee system alone does not meet the minimum standard of protection in roughly 25% of the SOW (the range across the scenarios is 21%–28%).

The 500-year flood protection suggested for critical infrastructure (1/500 mean annual exceedance probability) (p. 143, CPRA, 2017) is not met by the levee system alone in the ensemble median in any scenario (Figure 3, dashed yellow vertical line). In each of the three RCP8.5 scenarios combined with nonstationary storm surge (Figure 3, top three rows), about 65% of the SOW fail to meet this protection standard (the range across all scenarios is 61%–68%). No SOW in any scenario meets the economically efficient return level of 5000 years, as found by Jonkman et al. (2009) (Figure 3, dot–dashed blue vertical line).

The USACE is planning to raise much of this levee system by about 0.91 m (3 ft), in addition to other adaptive flood protection measures (USACE, 2014; Moritz et al., 2015). Even with the additional heightening, the levee system alone may still not be sufficient to attain required protection levels for critical infrastructure and will likely fall sizably short of economic efficiency (see Figure S1). The focus on the 50-year time horizon is motivated by the time horizon considered by the Coastal Protection and Restoration Authority of Louisiana (CPRA, 2017). This is relatively short compared to the time scale of the committed sea-level response. Recent work projecting future sea-level contributions from fast AIS dynamics confirms that the 50-year time horizon likely misses substantial sea-level contributions during the second half of this century (DeConto & Pollard, 2016; Bakker et al., 2017; Le Bars et al., 2017; Wong et al., 2017a). This underscores the

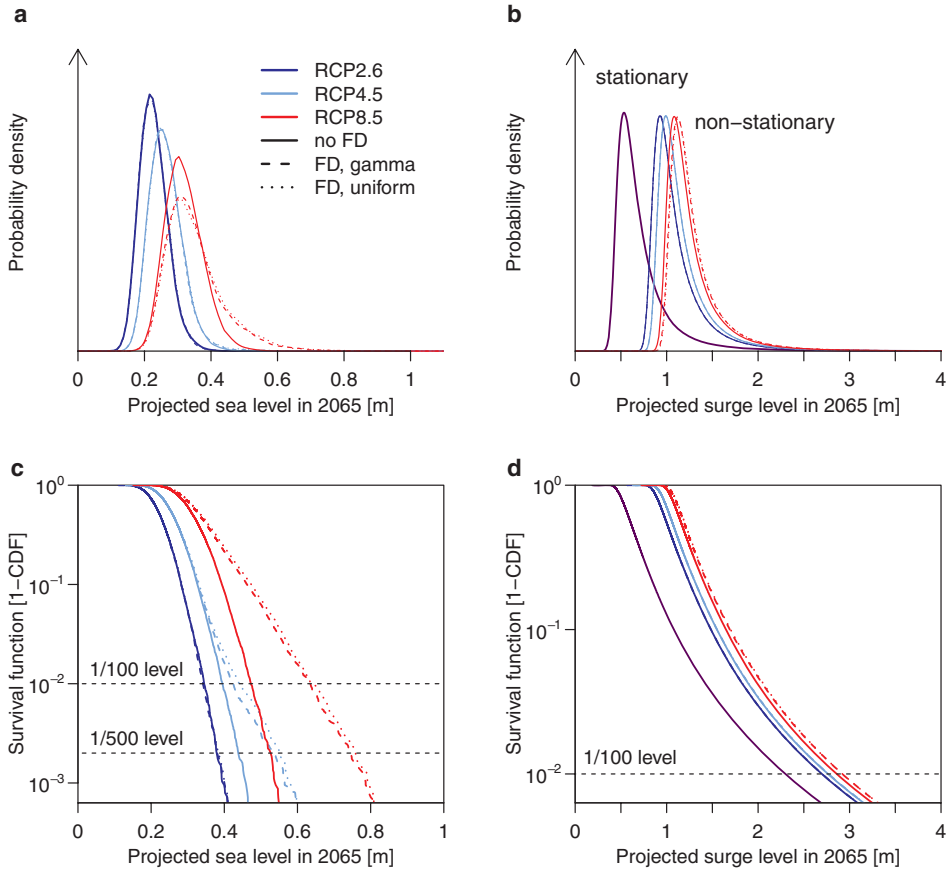

Figure 1. Probability density functions of (a) projected future sea level and (b) projected future storm surge levels, and (c, d) their associated survival functions (which give the total probability in the right tail of a distribution). "FD" refers to the fast Antarctic ice sheet dynamics; the dashed and dotted curves refer to the distributions obtained using the gamma and uniform prior distributions (respectively) for the fast dynamics parameters.

need for adaptive strategies for coastal risk management (Moritz et al., 2015). Previous work has demonstrated that a "future without action" fails to protect the Greater New Orleans area to the 100-year level by 2061 (Johnson et al., 2013). These authors considered a larger potential flood zone and uncertainty in system fragility beyond only overtopping of the levee system considered in the present work, which accounts for the differing estimates of system reliability. We note that the high-risk upper tail of our sea-level projections under RCP8.5 with fast Antarctic dynamics (c.f. Figure 1c) fall roughly between their "less-optimistic" and "high sea-level rise" scenarios of 45 cm and 78 cm sea-level rise over the 50-year time horizon.

3.3. Sensitivity Analysis

We find that the storm surge dominates the decomposition of variance in projected flood risk (Figure 4). The first-order sensitivity index for the shape parameter ξ of the storm surge GEV distribution accounts for 77% of the total variance in flood risk. This result is expected because the shape parameter determines the heaviness of the high-risk upper tail of the GEV distribution. This result is also in agreement with other recent assessments regarding the dominance of storm surge in flood risk uncertainty (Le Cozannet et al., 2015; Oddo et al., 2017). It is also difficult to constrain the shape parameter with observational data because extremal data are by definition rare. Other statistical approaches that make use of more data than the annual block maximum approach employed here may be of use to further constrain this parameter (e.g., monthly blocks or a Poisson process/generalized Pareto distribution approach (e.g., Tebaldi et al., 2012)). The first-order index for levee height ("build") accounts for another 8% of the flood risk variance. Perhaps not surprisingly, the total sensitivity index for "build" is 15%, demonstrating substantial interaction between levee heightening and other drivers of flood risk variability. Specifically, the second-order interaction index between "build" and the GEV shape parameter is 5% of the total variance in flood risk. The only other

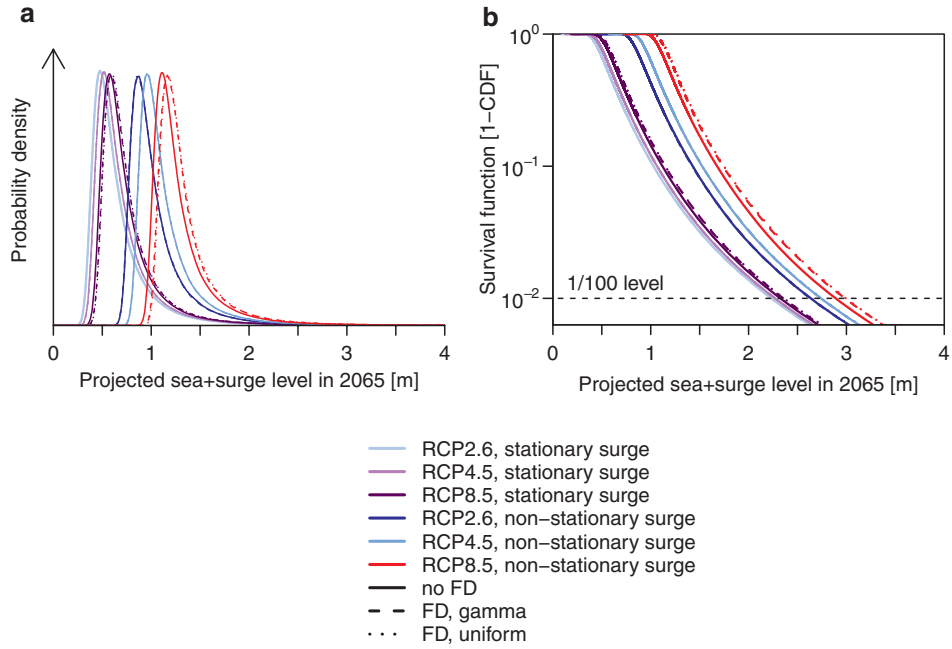

Figure 2. (a) Probability density functions and (b) survival functions for the 18 scenarios of radiative forcing, Antarctic ice sheet fast dynamics, and storm surge characterization. "FD" refers to the fast Antarctic ice sheet dynamics; the dashed and dotted curves refer to the distributions obtained using the gamma and uniform prior distributions (respectively) for the fast dynamics parameters.

statistically significant first-order sensitivity index is the scale parameter of the storm surge GEV distribution at 6% of the total flood risk variance.

The modeled global mean climate contributes substantially to the variance in flood risk via climate sensitivity (S, total sensitivity index of 25%), ocean vertical diffusivity (κ_D, 6%), and the interaction between the two (second-order interaction index of 3%). The simulated AIS dynamics drive variance in flood risk via ice sheet bed slope before loading ("slope", 37%), equilibrium runoff line height (h_0, 29%), runoff line height sensitivity to temperature (c, 27%), mean annual Antarctic precipitation (P_0, 9%), and a proportionality constant for ice flow speed at the ice sheet grounding line (f_0, 6%). We also find substantial interactions among the AIS parameters, ranging from 2% to 3% of the total flood risk variance.

4. Discussion and Caveats

This analysis is intended as didactic proof of concept and is silent on many likely important uncertainties. For example, we consider only a simple emulator of the fast AIS dynamical contributions to sea level (equation 1). Avenues to improve this analysis include considering an alternative model structure for this mechanism, potentially including a time-lagged response after the disintegration temperature has been reached. Our simple emulator also does not resolve contributions from the West Antarctic versus the East Antarctic ice sheets. This could be done by running two separately calibrated instances of the AIS model employed here and altering the assumed geometry, but is beyond the scope of the present work. Here, we focus on the potential impacts of the general Antarctic fast dynamics. Figure 2b demonstrates that this mechanism drives noticeable risks for New Orleans over the next 50 years, but Figure 4 highlights the fact that these AIS-driven risks are mild compared to those posed by storm surges.

The extrapolation of 36 years of tide gauge data to infer risks at the 1/100 or 1/500 level carries large uncertainties (e.g., NOAA, 2017). We further discuss the potential implications of this limited supply of data in Text S1, where we describe the following sensitivity experiment. We estimated the distributions of 100-year surge height using 37-year subsets of tide gauge data from Galveston, Texas, and Pensacola, Florida (the closest longer-duration tide gauge locations to New Orleans). We found that the results obtained from the Grand Isle record are qualitatively similar to the results we might expect from other similar-length data record from the U.S. Gulf Coast region. This ad hoc characterization of spatiotemporal

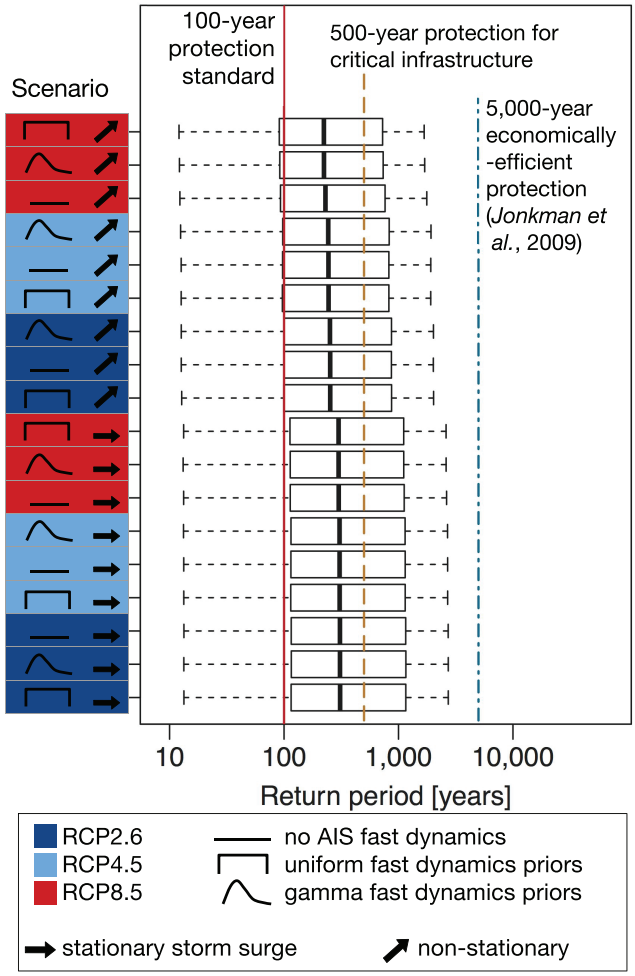

Figure 3. Return periods (inverse of flood probability) for the 18 scenarios, ordered from most severe (top) to least severe (bottom). The bold lines within each box denote the ensemble median; the extent of the boxes denotes the interquartile range (25%–75%); the extent of the horizontal dashed lines denotes the ensemble extrema; the solid red line denotes the 100-year protection standard; the dashed yellow line denotes the 500-year protection level for critical infrastructure (CPRA, 2017); and the blue dot–dashed line denotes the economically efficient protection level (Jonkman et al., 2009).

representation uncertainty is in line with previous work that finds strong heterogeneity in the spatial and temporal distributions of surge height estimates along the Gulf Coast (e.g., Buchanan et al., 2015). A wide and realistic representation of uncertainty is needed, however, to provide low-confidence (and more specifically, not overconfident) future projections to inform decision making (cf. Herman et al., 2015; Abadie et al., 2017). Indeed, across all of our scenarios, only 32%–39% of the SOW achieved the 500-year flood protection suggested for critical infrastructure, and about 72%–79% of the SOW achieved the 100-year flood protection standard (cf. Figure 3).

The results of the Sobol' sensitivity analysis indicate that the uncertainty in AIS dynamics and statistical characterization of the storm surge are key drivers of the flood risk variability. The design of effective flood risk management strategies (i.e., the exogenous levee heightening "build" term) would benefit from tighter constraint on these geophysical mechanisms. This may come in the form of assimilating expert judgment regarding future Antarctic mass loss (e.g., Oppenheimer et al., 2016) and consideration of alternative statistical approaches to characterize the storm surge level, for example, by leveraging new statistical models and improving the use of the limited data (e.g., Naveau et al., 2016; Stein, 2017).

The sensitivity analysis demonstrates that over the 2015–2065 project period considered here, the RCP scenario and rapid AIS dynamics (the parameters T_{crit} and λ) are not strongly linked to variance in future flood risk (Figure 4). This is attributed to the fact that the RCP scenarios do not substantially diverge by

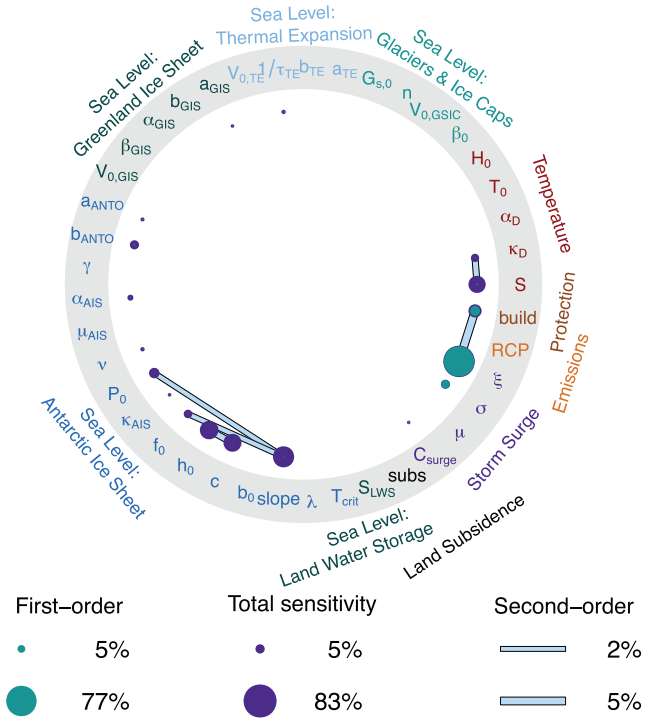

Figure 4. Sobol' sensitivity results for decomposition of the variance in projected flood risk over the 2015–2065 period (mean annual exceedance probability). Filled blue nodes represent first-order sensitivity indices; filled purple nodes represent total-order sensitivity indices; filled gray bars represent second-order sensitivity indices for the interaction between the parameter pair.

mid-century (Meinshausen et al., 2011). If one considers a time horizon of 2100, for example, then the RCP scenario and fast Antarctic mass loss likely play much larger roles. However, such a lengthy time horizon requires consideration of dynamic adaptive strategies for risk management in light of the deep uncertainties characterized here (Haasnoot et al., 2013; Quinn et al., 2017), as opposed to designing a long-term strategy at the beginning of the study period. This is another important avenue for future research.

Optimal levee designs indicate that the relative contributions of overtopping versus piping or slope instability failures to the total levee failure probability vary depending on site-specific properties, but overtopping is the dominant failure mode (Johnson et al., 2013; Bischiniotis et al., 2016). Our analysis considers overtopping to account for 100% of the total probability of failure and serves to provide an upper bound on the system reliability (Figure 4). We confirmed that our results are not significantly altered by prescribing overtopping to account for 60% or 80% of the total probability of failure, which is representative of the plausible range of failure modes (Bischiniotis et al., 2016) (see Figures S2 and S3). A more detailed probabilistic treatment of the different failure modes outlined here, as well as pumping system or floodgate failure, is beyond the scope of this study. As a simplification, we use a single elevation, sea level, storm surge level, subsidence rate, and levee height for the entire levee polder protecting the central metropolitan New Orleans area and do not consider non-levee forms of flood protection (e.g., elevated structures). More detailed modeling would be appropriate to inform on-the-ground decision making, accounting for local bathymetry, nonstructural protection measures, and levee system heterogeneity (e.g., Fischbach et al., 2012; Johnson et al., 2013). These caveats point to important research needs, as well as why these results should not be used to directly inform on-the-ground decisions.

5. Conclusions

Given these caveats, our results indicate a level of flood risk in New Orleans that, within 50 years, may well exceed the 500-year flood protection target for critical infrastructure. This protection target is missed by the levee system alone across all scenarios (in the ensemble median). The ensemble median in all scenarios achieves the 100-year flood protection standard, but about 25% of the SOW miss the 100-year flood protection standard (Figure 3). The storm surge characterization is found to be the primary driver of variance

in future flood risk, followed by AIS dynamics (Figure 4). These results highlight the importance of investing resources to determine the appropriate level of protection for a given levee system, as well as the need for further research on statistical models for extreme storm surge levels. Indeed, our results demonstrate how pursuing reduced emissions trajectories can lead to more successful flood risk management strategies by mitigating deeply uncertain risks across multiple system components.

Acknowledgments
We gratefully acknowledge Greg Garner, Robert Fuller, Kelsey Ruckert, Benjamin Lee, Vivek Srikrishnan, Alexander Bakker, Rob Lempert, David Johnson, and Neil Berg, as well as Bella and Chris Forest for invaluable inputs. This work was partially supported by the National Science Foundation through the Network for Sustainable Climate Risk Management (SCRiM) under NSF cooperative agreement GEO-1240507 as well as the Penn State Center for Climate Risk Management. The authors are not aware of any real or perceived conflicts of interest. Any conclusions or recommendations expressed in this material are those of the authors and do not necessarily reflect the views of the funding agencies. Any errors and opinions are, of course, those of the authors. All model codes, analysis codes, data, and model output used for analysis are freely available at https://github.com/scrim-network/BRICK/tree/scenarios. TW and KK initiated the study and designed the research. TW produced the model simulations, designed the initial figures, and wrote the first draft. Both contributed to the final text and figures.

References

Abadie, L. M., Galarraga, I., & de Murieta, E. S. (2017). Understanding risks in the light of uncertainty: low-probability, high-impact coastal events in cities. *Environmental Research Letters*, *12*(1), 14017. https://doi.org/10.1088/1748-9326/aa5254

Bakker, A. M. R., Wong, T. E., Ruckert, K. L., & Keller, K. (2017). Sea-level projections accounting for deeply uncertain ice-sheet contributions. *Scientific Reports*, *7*. https://doi.org/10.1038/s41598-017-04134-5

Bischiniotis, K., Kanning, W., Jonkman, S. N., & Kok, M. (2016). Cost-optimal design of river dikes using probabilistic methods. *Journal of Flood Risk Management*. https://doi.org/10.1111/jfr3.12277

Bryant, B. P., & Lempert, R. J. (2010). Thinking inside the box: A participatory, computer-assisted approach to scenario discovery. *Technological Forecasting and Social Change*, *77*(1), 34–49. https://doi.org/10.1016/j.techfore.2009.08.002

Buchanan, M. K., Kopp, R. E., Oppenheimer, M., & Tebaldi, C. (2015). Allowances for evolving coastal flood risk under uncertain local sea-level rise. *Climatic Change*, *137*(3–4), 347–362. https://doi.org/10.1007/s10584-016-1664-7.

Butler, M. P., Reed, P. M., Fisher-Vanden, K., Keller, K., & Wagener, T. (2014). Identifying parametric controls and dependencies in integrated assessment models using global sensitivity analysis. *Environmental Modelling and Software*, *59*, 10–29. https://doi.org/10.1016/j.envsoft.2014.05.001

Coastal Protection and Restoration Authority (CPRA) (2017). *Louisiana's Comprehensive Master Plan for a Sustainable Coast*. Baton Rouge, LA: Coastal Protection and Restoration Authority of Louisiana.

R Core Team (2016). *R: A Language and Environment for Statistical Computing*. Vienna: Austria.

De Winter, R., Reerink, T. J., Slangen, A. B. A., De Vries, H., Edwards, T., & Van De Wal, R. S. W. (2017). Impact of asymmetric uncertainties in ice sheet dynamics on regional sea level projections. *Natural Hazards and Earth System Sciences*, (April), 1–25. https://doi.org/10.5194/nhess-2017-86

DeConto, R. M., & Pollard, D. (2016). Contribution of Antarctica to past and future sea-level rise. *Nature*, *531*, 591–597. https://doi.org/10.1038/nature17145

Diaz, D., & Keller, K. (2016). A potential disintegration of the West Antarctic Ice Sheet: Implications for economic analyses of climate policy. *The American Economic Review*, *106*(5), 607–611. https://doi.org/10.1257/aer.p20161103

Dixon, T. H., Amelung, F., Ferretti, A., Novali, F., Rocca, F., Dokka, R., Sella, G., Kim, S.-W., Wdowinski, S., & Whitman, D. (2006). Space geodesy: Subsidence and flooding in New Orleans. *Nature*, *441*(7093), 587–588. https://doi.org/10.1038/441587a

Fischbach, J. R., Johnson, D. R., Ortiz, D. S., Bryant, B. P., Hoover, M., & Ostwald, J. (2012). *Coastal Louisiana Risk Assessment Model: Technical Description and 2012 Coastal Master Plan Analysis Results*. CA, USA: Santa Monica.

Gilleland, E., Ribatet, M., & Stephenson, A. G. (2013). A software review for extreme value analysis. *Extremes*, *16*(1), 103–119. https://doi.org/10.1007/s10687-012-0155-0

Grinsted, A., Moore, J. C., & Jevrejeva, S. (2013). Projected Atlantic hurricane surge threat from rising temperatures. *Proceedings of the National Academy of Sciences of the United States of America*, *110*(14), 5369–5373. https://doi.org/10.1073/pnas.1209980110

Haasnoot, M., Kwakkel, J. H., Walker, W. E., & ter Maat, J. (2013). Dynamic adaptive policy pathways: A method for crafting robust decisions for a deeply uncertain world. *Global Environmental Change*, *23*(2), 485–498. https://doi.org/10.1016/j.gloenvcha.2012.12.006

Hallegatte, S., Green, C., Nicholls, R. J., & Corfee-Morlot, J. (2013). Future flood losses in major coastal cities. *Nature Climate Change*, *3*(9), 802–806. https://doi.org/10.1038/nclimate1979

Herman, J., Reed, P., Zeff, H., & Characklis, G. (2015). How Should Robustness Be Defined for Water Systems Planning under Change? *Journal of Water Resources Planning and Management*, *141*(10), 4015012. https://doi.org/10.1061/(ASCE)WR.1943-5452.0000509.

Hinkel, J., Jaeger, C., Nicholls, R. J., Lowe, J., Renn, O., & Peijun, S. (2015). Sea-level rise scenarios and coastal risk management. *Nature Climate Change*, *5*(3), 188–190. https://doi.org/10.1038/nclimate2505

Hinkel, J., Lincke, D., Vafeidis, A. T., Perrette, M., Nicholls, R. J., Tol, R. S. J., Marzeion, B., Fettweis, X., Ionescu, C., & Levermann, A. (2014). Coastal flood damage and adaptation costs under 21st century sea-level rise. *Proceedings of the National Academy of Sciences of the United States of America*, *111*(9), 3292–3297. https://doi.org/10.1073/pnas.1222469111

Jackson, L. P., & Jevrejeva, S. (2016). A probabilistic approach to 21st century regional sea-level projections using RCP and high-end scenarios. *Global and Planetary Change*, *146*, 179–189. https://doi.org/10.1016/j.gloplacha.2016.10.006

Janon, A., Klein, T., Lagnoux, A., Nodet, M., & Prieur, C. (2014). Asymptotic normality and efficiency of two Sobol index estimators. *ESAIM: Probability and Statistics*, *18*(3), 342–364. https://doi.org/10.1051/ps/2013040

Johnson, D. R., Fischbach, J. R., & Ortiz, D. S. (2013). Estimating Surge-Based Flood Risk with the Coastal Louisiana Risk Assessment Model. *Journal of Coastal Research*, *67*, 109–126. https://doi.org/10.2112/SI_67_8

Jonkman, S. N., Kok, M., van Ledden, M., & Vrijling, J. K. (2009). Risk-based design of flood defence systems: a preliminary analysis of the optimal protection level for the New Orleans metropolitan area. *Journal of Flood Risk Management*, *2*(3), 170–181. https://doi.org/10.1111/j.1753-318X.2009.01036.x

Kopp, R., DeConto, R. M., Bader, D., Horton, R. M., Hay, C. C., Kulp, S., Oppenheimer, M., Pollard, D., & Strauss, B. H. (2017). Implications of ice-shelf hydrofracturing and ice cliff collapse mechanisms for sea-level projections. *Atmospheric and Oceanic Physics* https://arxiv.org/abs/1704.05597

Kopp, R. E., Horton, R. M., Little, C. M., Mitrovica, J. X., Oppenheimer, M., Rasmussen, D. J., Strauss, B. H., & Tebaldi, C. (2014). Probabilistic 21st and 22nd century sea-level projections at a global network of tide-gauge sites. *Earth's Future*, *2*(8), 383–406. https://doi.org/10.1002/2014EF000239

Kopp, R. E., Kemp, A. C., Bittermann, K., Horton, B. P., Donnelly, J. P., Gehrels, W. R., Hay, C. C., Mitrovica, J. X., Morrow, E. D., & Rahmstorf, S. (2016). Temperature-driven global sea-level variability in the Common Era. *Proceedings of the National Academy of Sciences of the United States of America*, *113*(11), E1434–E1441. https://doi.org/10.1073/pnas.1517056113

Langlois, R. N., & Cosgel, M. M. (1993). Frank Knight on Risk, Uncertainty, and the Firm: A New Interpretation. *Economic Inquiry*, *31*(3), 456–465. https://doi.org/10.1111/j.1465-7295.1993.tb01305.x

Le Bars, D., Drijfhout, S., & de Vries, H. (2017). A high-end sea level rise probabilistic projection including rapid Antarctic ice sheet mass loss. *Environmental Research Letters*, *39*(4), 51230. https://doi.org/10.1088/1748-9326/aa6512
Le Cozannet, G., Rohmer, J., Cazenave, A., Idier, D., van de Wal, R., de Winter, R., Pedreros, R., Balouin, Y., Vinchon, C., & Oliveros, C. (2015). Evaluating uncertainties of future marine flooding occurrence as sea-level rises. *Environmental Modelling and Software*, *73*, 44–56. https://doi.org/10.1016/j.envsoft.2015.07.021
Lempert, R., Sriver, R. L., & Keller, K. (2012). *Characterizing Uncertain Sea Level Rise Projections to Support Investment Decisions*. Santa Monica, CA: California Energy Commission; Publication Number: CEC-500-2012-056.
Lima, M. (2011). *Visual Complexity: Mapping Patterns of Information*. New York: Princeton Architectural Press.
Little, C. M., Horton, R. M., Kopp, R. E., Oppenheimer, M., Vecchi, G. A., & Villarini, G. (2015). Joint projections of US East Coast sea level and storm surge. *Nature Climate Change*, *5*(September), 1114–1120. https://doi.org/10.1038/nclimate2801
Meinshausen, M., et al. (2011). The RCP greenhouse gas concentrations and their extensions from 1765 to 2300. *Climatic Change*, *109*(1–2), 213–241. https://doi.org/10.1007/s10584-011-0156-z
Moftakhari, H. R., AghaKouchak, A., Sanders, B. F., & Matthew, R. A. (2017). Cumulative hazard: The case of nuisance flooding. *Earth's Future*, *5*(2), 214–223. https://doi.org/10.1002/2016EF000494
Moritz, H., et al. (2015). USACE adaptation approach for future coastal climate conditions. *Proceedings of the Institution of Civil Engineers: Maritime Engineering*, *168*(3), 111–117. https://doi.org/10.1680/jmaen.15.00015
Naveau, P., Huser, R., Ribereau, P., & Hannart, A. (2016). Modeling jointly low, moderate, and heavy rainfall intensities without a threshold selection. *Water Resources Research*, *52*, 2753–2769. https://doi.org/10.1002/2015WR018552
Nicholls, R. J., & Cazenave, A. (2010). Sea level rise and its impact on coastal zones. *Science*, *328*(5985), 1517–1520. https://doi.org/10.1126/science.1185782
NOAA (2017), NOAA Tides and Currents: Grand Isle, LA - Station ID: 8761724. National Oceanic and Atmospheric Administration (NOAA), accessed Jan 11, 2017 (Available at https://tidesandcurrents.noaa.gov/stationhome.html?id=8761724.)
Oddo, P. C., Lee, B. S., Garner, G. G., Srikrishnan, V., Reed, P. M., Forest, C. E., & Keller, K. (2017). Deep uncertainties in sea-level rise and storm surge projections: Implications for coastal flood risk management. *Risk Analysis*. https://doi.org/10.1111/risa.12888
Oppenheimer, M., & Alley, R. B. (2016). How high will the seas rise? *Science*, *354*(6318), 1375–1377. https://doi.org/10.1126/science.aak9460
Oppenheimer, M., Little, C. M., & Cooke, R. M. (2016). Expert judgement and uncertainty quantification for climate change. *Nature Climate Change*, *6*(5), 445–451. https://doi.org/10.1038/nclimate2959
Orton, P. M., Hall, T. M., Talke, S. A., Blumberg, A. F., Georgas, N., & Vinogradov, S. (2016). A validated tropical-extratropical flood hazard assessment for New York Harbor. *Journal of Geophysical Research, Oceans*, *121*. https://doi.org/10.1002/2014JC011679
Quinn, J. D., Reed, P. M., & Keller, K. (2017). Direct policy search for robust multi-objective management of deeply uncertain socio-ecological tipping points. *Environmental Modelling and Software*, *92*, 125–141. https://doi.org/10.1016/j.envsoft.2017.02.017
Ray, R. D., & Foster, G. (2016). Future nuisance flooding at Boston caused by astronomical tides alone. *Earth's Future*, *4*(12), 578–587. https://doi.org/10.1002/2016EF000423
Resio, D. T., Irish, J. L., Westerink, J. J., & Powell, N. J. (2013). The effect of uncertainty on estimates of hurricane surge hazards. *Natural Hazards*, *66*(3), 1443–1459. https://doi.org/10.1007/s11069-012-0315-1
Ritz, C., Edwards, T. L., Durand, G., Payne, A. J., Peyaud, V., & Hindmarsh, R. C. A. (2015). Potential sea-level rise from Antarctic ice-sheet instability constrained by observations. *Nature*, *528*(7580), 115–118. https://doi.org/10.1038/nature16147.
Ruckert, K. L., Shaffer, G., Pollard, D., Guan, Y., Wong, T. E., Forest, C. E., & Keller, K. (2017). Assessing the impact of retreat mechanisms in a simple Antarctic ice sheet model using Bayesian calibration. *PLoS One*, *12*(1), e0170052. https://doi.org/10.1371/journal.pone.0170052
Saltelli, A. (2002). Making best use of model evaluations to compute sensitivity indices. *Computer Physics Communications*, *145*(2), 280–297. https://doi.org/10.1016/S0010-4655(02)00280-1
Schoemaker, P. J. H. (1993). Multiple scenario development: Its conceptual and behavioral foundation. *Strategic Management Journal*, *14*(3), 193–213. https://doi.org/10.1002/smj.4250140304
Slangen, A. B. A., Carson, M., Katsman, C. A., van de Wal, R. S. W., Köhl, A., Vermeersen, L. L. A., & Stammer, D. (2014). Projecting twenty-first century regional sea-level changes. *Climatic Change*, *124*(1–2), 317–332. https://doi.org/10.1007/s10584-014-1080-9
Sobol', I. M. (2001). Global sensitivity indices for nonlinear mathematical models and their Monte Carlo estimates. *Mathematics and Computers in Simulation*, *55*(1–3), 271–280. https://doi.org/10.1016/S0378-4754(00)00270-6
Stein, M. L. (2017). Should annual maximum temperatures follow a generalized extreme value distribution? *Biometrika*, *104*(1), 1–16. https://doi.org/10.1093/biomet/asw070
Sweet, W. V., & Park, J. (2014). From the extreme to the mean: Acceleration and tipping points of coastal inundation from sea level rise. *Earth's Future*, *2*(12), 579–600. https://doi.org/10.1002/2014EF000272
Tebaldi, C., Strauss, B. H., & Zervas, C. E. (2012). Modelling sea level rise impacts on storm surges along US coasts. *Environmental Research Letters*, *7*(1), 14032. https://doi.org/10.1088/1748-9326/7/1/014032.
United States Army Corps of Engineers (USACE) (2012), Hurricane and Storm Damage Risk Reduction System Design Guidelines, New Orleans District.
United States Army Corps of Engineers (USACE) (2014), Elevations for Design of Hurricane Protection Levees and Structures, New Orleans District.
Urban, N. M., & Keller, K. (2010). Probabilistic hindcasts and projections of the coupled climate, carbon cycle and Atlantic meridional overturning circulation system: a Bayesian fusion of century-scale observations with a simple model. *Tellus A*, *62*(5), 737–750. https://doi.org/10.1111/j.1600-0870.2010.00471.x
Vandenberg-Rodes, A., Moftakhari, H. R., AghaKouchak, A., Shahbaba, B., Sanders, B. F., & Matthew, R. A. (2016). Projecting nuisance flooding in a warming climate using generalized linear models and Gaussian processes. *Journal of Geophysical Research, Oceans*, *121*(11), 8008–8020. https://doi.org/10.1002/2016JC012084
Walker, W. E., Haasnoot, M., & Kwakkel, J. H. (2013). Adapt or perish: A review of planning approaches for adaptation under deep uncertainty. *Sustainability*, *5*(3), 955–979. https://doi.org/10.3390/su5030955
Wong, T. E., Bakker, A. M. R., & Keller, K. (2017a). Impacts of Antarctic fast dynamics on sea-level projections and coastal flood defense. *Climatic Change*, *144*(2). https://doi.org/10.1007/s10584-017-2039-4
Wong, T. E., Bakker, A. M. R., Ruckert, K. L., Applegate, P., Slangen, A., & Keller, K. (2017b). BRICK0.2, a simple, accessible and transparent model framework for climate and sea-level projections. *Geoscientific Model Development*, *10*, 2741–2760. https://doi.org/10.5194/gmd-10-2741-2017